On the Performance of Transmitted-Reference Impulse Radio

Sinan Gezici[1], *Student Member, IEEE,* Fredrik Tufvesson[2], *Member, IEEE,* and Andreas F. Molisch[2,3], *Senior Member, IEEE*

[1]Dept. of Electrical Engineering
Princeton University
Princeton, NJ 08544, USA
Email: sgezici@princeton.edu

[2]Dept. of Electroscience
Lund University
Box 118, SE-221 00 Lund, Sweden
Email: fredrik.tufvesson@es.lth.se

[3]Mitsubishi Electric Research Labs
201 Broadway
Cambridge, MA 02139, USA
Email: andreas.molisch@ieee.org

***Abstract*— We consider a time-hopping impulse-radio system that uses transmitted-reference pulses for implicit channel estimation and equalization. A hybrid receiver structure first performs a filtering matched to the hopping sequence, and a subsequent correlation of the data pulses with the reference pulses. We analyze the performance of such a system both in AWGN and in multipath. For the AWGN case, we give exact expressions for the bit error probability that take into account the non-Gaussian nature of the noise-noise crossterms arising in the correlators. For the multipath case, we analyze inter-frame interference, as well as multipath interference from the reference pulse to the data pulse, providing closed-form equations in the limit of a large number of multipath components.**

I. Introduction

In recent years, ultrawideband (UWB) communications, where the signal occupies more than 20% relative bandwidth, or more than 500 MHz absolute bandwidth, has raised enormous interest in the academic, industrial, and military community. Time-hopping impulse radio (TH-IR) is a UWB modulation and multiple-access scheme that is especially well suited for low-data-rate communications, and has been intensively studied since the pioneering work of Win and Scholtz [1], [2]. TH-IR is also a leading candidate for the IEEE 802.15.4a standard for low-data-rate communications. In TH-IR, each symbol is represented by a sequence of short pulses. Each symbol duration is subdivided into a number of *frames*, where each frame carries one pulse. The position of the pulse within the frame is determined by a pseudorandom sequence, and different users use different sequences. Thus, even for unsynchronized users, at most one pulse per symbol can "collide" (arrive at the receiver simultaneously). The time-hopping thus guarantees the multiple-access performance. The use of short pulses within each frame provides the spectral spreading, resulting in the high bandwidth that is characteristic for UWB systems.

The short pulses also result in a very high delay resolution. This is helpful for the reduction of fading when optimum receiver structures (all-Rake receivers) are used [3]. However, it does lead to a reduction of the received *total* energy when suboptimum receiver structures, like partial Rake receivers, are used [4], [5]. For this reason, transmitted-reference (TR) schemes have become popular [5]-[8]. In a TR scheme, two transmitted pulses are used in each frame. The first pulse is not modulated (i.e., does not carry information about the data) and is called the reference pulse. The second pulse, which is modulated, is separated by a time delay T_d from the first pulse, and is called the data pulse. The receiver uses pulse-pair correlators to recover the data, thus performing channel estimation and despreading in one simple step. Each multipath component results in a peak at the output of the multiplier with the same phase (which is determined by the value of the data symbol), and therefore they can be summed by an integrator over a certain period. The integrator output is detected in a conventional way to make a decision on the transmitted data symbols.

A major drawback of the TR scheme is the excess noise related to the multiplication of noise contributions in the received reference pulses with the noise contributions in the received data pulses. In a recent paper [9], the authors have suggested a new transceiver structure that reduces the noise-noise cross terms, and have given an approximate analysis of its performance. In this paper, we perform a more in-depth mathematical analysis of this structure; however we note that the performance of "conventional" TR receivers can be obtained from our analysis as a special case. Specifically, we analyze the impact of the non-Gaussian nature of the noise-noise cross terms, as well as the inter-frame interference (IFI) and the reference-pulse-on-data-pulse interference in multipath environments. None of those aspects have, to our knowledge, been treated in previous papers on UWB TR schemes.

The remainder of the paper is organized the following way: Section II describes the system setup and establishes the notation. Section III analyzes the bit error probability (BEP) performance over AWGN channels. Subsequently, the performance in delay-dispersive multipath channels is analyzed in Section IV, and the theoretical results are compared with simulation results. A summary and conclusions wraps up the paper.

II. System model

The transmit signal uses TH-IR as multiple access format, and TR BPSK as modulation format. The transmit signal can

 0-7803-8794-5/04/$20.00

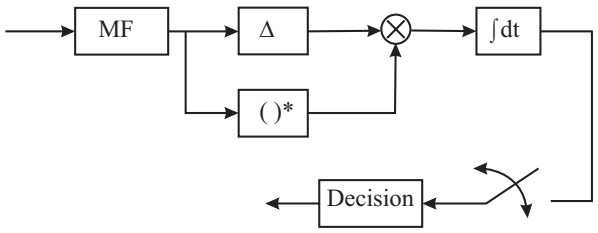

Fig. 1. Building blocks for the basic hybrid receiver. Note that the sampling circuit performs symbol rate sampling.

thus be written as

$$s_{TX}(t) = \sqrt{\frac{E_s}{2N_f}} \sum_{j=-\infty}^{\infty} d_j [w_{tx}(t - jT_f - c_j T_c) + b_{\lfloor j/N_f \rfloor} w_{tx}(t - jT_f - c_j T_c - T_d)], \quad (1)$$

where T_c denotes the chip duration, T_f is the frame duration, and T_d is the delay between the reference pulse and the data pulse. We assume that $T_d = \Delta T_c$, where Δ is a positive integer. The c_j denote a (pseudo-)random integer sequence with values between 0 and $N_c - 1$, which determines the time-hopping sequence, with N_c being the number of chips per frame. The d_j denote a pseudorandom sequence of $\{-1, +1\}$ that ensures a zero-mean output and is also helpful in the shaping of the transmit spectrum [10] according to the FCC rules [11]. The function $w_{tx}(t)$ denotes the transmit waveform; in the following, we assume that its support extends only over one chip duration. E_s is the energy per transmitted symbol. Note that $T_s = N_f T_f$ is the symbol duration.

Let $r(t)$ denote the received signal. The first step at the receiver, shown in Figure 1, is to pass $r(t)$ through a matched filter matched to the following template signal for the ith information bit:

$$s_{temp}^{(i)}(t) = \frac{1}{\sqrt{N_f}} \sum_{j=iN_f}^{(i+1)N_f - 1} d_j w_{rx}(t - jT_f - c_j T_c), \quad (2)$$

where $w_{rx}(t)$ denotes the received UWB pulse.

Then, the output of the matched filter can be expressed as

$$\tilde{r}(t) = \int r(\tau) s_{temp}^{(i)}(\tau - t) d\tau. \quad (3)$$

III. Transmission over AWGN Channels

When $s_{TX}(t)$ in (1) is transmitted over an AWGN channel, the received signal $r(t)$ can be expressed as:

$$r(t) = \sqrt{\frac{E_s \alpha}{2N_f}} \sum_{j=-\infty}^{\infty} d_j [w_{rx}(t - jT_f - c_j T_c) + b_{\lfloor j/N_f \rfloor} w_{rx}(t - jT_f - c_j T_c - T_d)] + \sigma_n n(t), \quad (4)$$

where α is the channel attenuation, and $n(t)$ is a zero mean white Gaussian process with unit spectral density. Depending on whether we consider a baseband or bandpass filter, $n(t)$ is a real or complex Gaussian process, respectively.

The estimator in the AWGN case can be expressed as

$$\hat{b}_i = \text{sign}\{\tilde{r}(0)\tilde{r}(T_d)\}, \quad (5)$$

where $\tilde{r}(t)$ is the output of the matched filter as shown in (3). The following lemma expresses the probability distribution of the decision variable under some conditions.

Lemma 3.1: Assume that the TH sequence is constrained to the set $\{0, 1, \ldots, N_m - 1\}$, where $N_m = N_c - \Delta - 1$, with $\Delta = T_d/T_c$ being an integer. Then, the decision variable can be expressed as

$$\tilde{r}(0)\tilde{r}(T_d) = b_i R^2(0) \frac{E_s \alpha}{2} + N, \quad (6)$$

where $R(t) = \int_{-\infty}^{\infty} w_{rx}(\tau) w_{rx}(\tau - t) d\tau$, and the conditional distribution of N given the information bit b_i is given by

$$p_N(n|b_i) = \frac{1}{2\pi\sigma_n^2 R(0)} \int_{-\infty}^{\infty} \frac{1}{|z + cb_i|} \times \exp\left\{ -\frac{1}{2\sigma_n^2 R(0)} \left[\frac{(n - cz)^2}{(z + cb_i)^2} + z^2 \right] \right\} dz, \quad (7)$$

with $c := \sqrt{\frac{E_s \alpha}{2}} R(0)$.

Proof: See [12].

Assuming equiprobable information bits, the BEP can be calculated from (6) as

$$P_e = 0.5 \int_{-\infty}^{0} p_N\left(n - 0.5\alpha E_s R^2(0) \,|\, b_i = +1\right) dn + 0.5 \int_{0}^{\infty} p_N\left(n + 0.5\alpha E_s R^2(0) \,|\, b_i = -1\right) dn. \quad (8)$$

Then, using (7), the following BEP expression can be obtained after some manipulation:

$$P_e = \frac{1}{\sqrt{2\pi R(0)\sigma_n^2}} \int_{-\infty}^{\infty} e^{-\frac{z^2}{2\sigma_n^2 R(0)}} Q\left(\frac{cz + 0.5\alpha E_s R^2(0)}{\sqrt{R(0)\sigma_n^2}\,|z + c|} \right) dz, \quad (9)$$

where $Q(x) = \frac{1}{\sqrt{2\pi}} \int_x^{\infty} e^{-t^2/2} dt$.

To confirm and illustrate the results, we performed Monte Carlo simulations of a TR scheme in an AWGN channel. Figure 2 shows the results of those simulations and compares them to the evaluations of (9), where a good agreement between the theory and simulations is observed. Also the performance of the optimum receiver is shown in the plot for comparison purposes.

IV. Transmission over Frequency-Selective Channels

A. Channel Model

We consider the following channel model

$$h(t) = \sum_{l=0}^{L-1} a_l \delta(t - lT_c), \quad (10)$$

where L is the number of multipaths and a_l is the fading coefficient of the lth path with $\sum_{l=0}^{L-1} a_l^2 = 1$.

The following assumptions are made in order to facilitate the theoretical analysis:

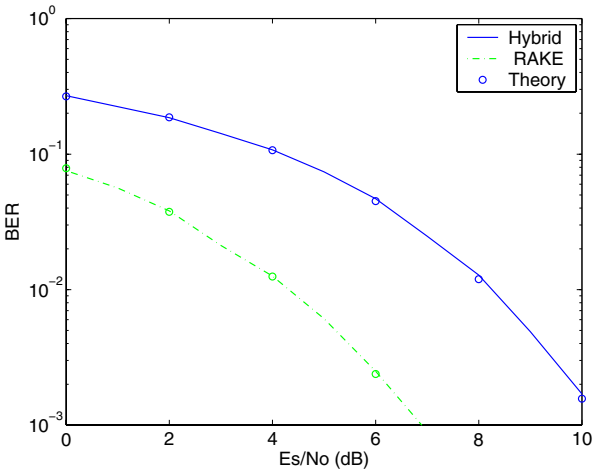

Fig. 2. BEP as a function of the signal-to-noise ratio for optimum (Rake) receiver and the hybrid receiver. Solid curves are the Monte Carlo simulations, and the curves with circle marks are the theoretical results; i.e., evaluation of (9). The Monte Carlo simulations and the theoretical curves completely overlap.

- There is a guard interval between the symbols so that no inter-symbol interference (ISI) exists.
- The TH sequence c_j in (1) is constrained to the set $\{0, 1, \ldots, N_m - 1\}$, where $N_m = N_c - Q - 1$, with Q being a positive integer determining the integration interval as will be defined later in this section.

B. General Theory

From (1) and (10), the received signal can be expressed as

$$r(t) = \sqrt{\frac{E_s\alpha}{2N_f}} \sum_{j=-\infty}^{\infty} \sum_{l=0}^{L-1} a_l d_j [w_{rx}(t - jT_f - c_jT_c - lT_c) + b_{\lfloor j/N_f \rfloor} w_{rx}(t - jT_f - c_jT_c - T_d - lT_c)] + \sigma_n n(t). \quad (11)$$

Using $r(t)$ in (11) and the template signal in (2), the despread signal $\tilde{r}(t)$ in (3) can be expressed as

$$\tilde{r}(t) = \sqrt{\frac{E_s\alpha}{2N_f^2}}\, f_{b_i}(t) + \frac{\sigma_n}{\sqrt{N_f}}\, n_w(t), \quad (12)$$

where

$$f_{b_i}(t) := \sum_{j=iN_f}^{(i+1)N_f-1} \sum_{j'=iN_f}^{(i+1)N_f-1} \sum_{l=0}^{L-1} a_l d_j d_{j'} \times \{R[t + (j' - j)T_f + (c_{j'} - c_j)T_c - lT_c] + b_i R[t + (j' - j)T_f + (c_{j'} - c_j)T_c - T_d - lT_c]\} \quad (13)$$

and

$$n_w(t) := \int_{-\infty}^{\infty} g(\tau - t) n(\tau) d\tau, \quad (14)$$

with

$$g(t) := \sum_{j=iN_f}^{(i+1)N_f-1} d_j w_{rx}(t - jT_f - c_jT_c). \quad (15)$$

The decision is given by the following:

$$\hat{b}_i = \text{sign}\left\{ \int_{T_d - T_c}^{T_d + QT_c} \tilde{r}(t)\tilde{r}(t - T_d) dt \right\}, \quad (16)$$

where Q is the integer that determines the integration interval, and the decision variable can be expressed as

$$\int_{T_d - T_c}^{T_d + QT_c} \tilde{r}(t)\tilde{r}(t - T_d) dt = S_{b_i} + N_1 + N_2, \quad (17)$$

where S_{b_i} is the signal part, N_1 is the noise-noise term and N_2 is the signal-noise term.

The signal part S_{b_i} can be expressed as

$$S_{b_i} = \frac{E_s\alpha}{2N_f^2} \int_{T_d - T_c}^{T_d + QT_c} f_{b_i}(t) f_{b_i}(t - T_d) dt, \quad (18)$$

where $f_{b_i}(t)$ is as in (13).

The noise-noise term N_1 in (17) is given by

$$N_1 = \frac{\sigma_n^2}{N_f} \int_{T_d - T_c}^{T_d + QT_c} n_w(t) n_w(t - T_d) dt, \quad (19)$$

the distribution of which can be approximated as shown in the following lemma:

Lemma 4.1: As $Q \longrightarrow \infty$, $N_1/\sqrt{Q+1}$ is asymptotically normally distributed as

$$\mathcal{N}\left(0\,,\, \frac{\sigma_n^4}{N_f^2} \int_{-\infty}^{\infty} \int_{-\infty}^{\infty} [l_q^2(\tau, \hat{\tau}) + 2 l_q(\tau, \hat{\tau}) l_{q+1}(\tau, \hat{\tau})] d\tau d\hat{\tau}\right), \quad (20)$$

where

$$l_q(\tau, \hat{\tau}) := \int_{T_d + (q-1)T_c}^{T_d + qT_c} g(\tau - t) g(\hat{\tau} - t + T_d) dt. \quad (21)$$

Proof: See [12].

The signal-noise term N_2 in (17) is expressed as

$$N_2 = \frac{\sigma_n}{N_f} \sqrt{\frac{E_s\alpha}{2N_f}} \int_{T_d - T_c}^{T_d + QT_c} [f_{b_i}(t) n_w(t - T_d) + n_w(t) f_{b_i}(t - T_d)] dt. \quad (22)$$

Using (22), (14), and the fact that $n(t)$ is a white Gaussian process, we obtain the distribution of N_2 as

$$N_2 \sim \mathcal{N}\left(0\,,\, \frac{\sigma_n^2 E_s\alpha}{2N_f^3} \int_{-\infty}^{\infty} [h_{b_i}(\tau; 0, T_d) + h_{b_i}(\tau; T_d, 0)]^2 d\tau\right), \quad (23)$$

where

$$h_{b_i}(\tau; x, y) := \int_{T_d - T_c}^{T_d + QT_c} f_{b_i}(t - x) g(\tau - t + y) dt. \quad (24)$$

Now consider the total noise $N = N_1 + N_2$. It can be shown from (19) and (22) that N_1 and N_2 are uncorrelated. Hence, the approximate distribution of the total noise N can be obtained from (20) and (23) as

$$N \sim \mathcal{N}\left(0\,,\, \frac{\sigma_n^4 (Q+1)}{N_f^2}\, \sigma_1^2 + \frac{\sigma_n^2 E_s\alpha}{2N_f^3}\, \sigma_2^2(b_i)\right), \quad (25)$$

where

$$\sigma_1^2 := \int_{-\infty}^{\infty}\int_{-\infty}^{\infty}[l_q^2(\tau,\hat{\tau}) + 2l_q(\tau,\hat{\tau})l_{q+1}(\tau,\hat{\tau})]d\tau d\hat{\tau}, \tag{26}$$

$$\sigma_2^2(b_i) := \int_{-\infty}^{\infty}[h_{b_i}(\tau;0,T_d) + h_{b_i}(\tau;T_d,0)]^2 d\tau. \tag{27}$$

Since the decision variable in (17) is equal to $S_{b_i}+N$ with S_{b_i} given by (18), the BEP is obtained as

$$P_e = 0.5\,Q\left(\frac{0.5E_s\alpha\int_{T_d-T_c}^{T_d+QT_c} f_{+1}(t)f_{+1}(t-T_d)dt}{\sqrt{N_f^2\sigma_n^4(Q+1)\,\sigma_1^2 + 0.5N_f\sigma_n^2E_s\alpha\,\sigma_2^2(1)}}\right) + 0.5\,Q\left(\frac{-0.5E_s\alpha\int_{T_d-T_c}^{T_d+QT_c} f_{-1}(t)f_{-1}(t-T_d)dt}{\sqrt{N_f^2\sigma_n^4(Q+1)\,\sigma_1^2 + 0.5N_f\sigma_n^2E_s\alpha\,\sigma_2^2(-1)}}\right). \tag{28}$$

C. Special Case: No Inter-frame Interference

If the frames are spaced sufficiently apart, there occurs no IFI. However, there can still be interference from the reference pulses to the data pulses, as those are typically closely spaced together.

Assume that $N_m \le N_c - \Delta - \max\{Q, L\}$. Then, $f_{b_i}(t)$ in (13) can be expressed as follows:

$$f_{b_i}(t) = N_f\sum_{l=0}^{L-1} a_l[R(t-lT_c) + b_iR(t-(\Delta+l)T_c)]. \tag{29}$$

Hence, the signal part is given by

$$S_{b_i} = \frac{E_s\alpha}{2}[(S_1+S_2) + b_i(S_3+S_4)], \tag{30}$$

where S_1, S_2, S_3 and S_4 can be shown to be given by

$$S_1 = \sum_{q=0}^{Q}[A(a_{q-1}a_{q+\Delta-1} + a_qa_{q+\Delta}) + C(a_qa_{q+\Delta-1} + a_{q-1}a_{q+\Delta})], \tag{31}$$

$$S_2 = \sum_{q=0}^{Q}[A(a_{q-1}a_{q-\Delta-1} + a_qa_{q-\Delta}) + C(a_{q-1}a_{q-\Delta} + a_qa_{q-\Delta-1})], \tag{32}$$

$$S_3 = \sum_{q=0}^{Q}[A(a_{q+\Delta-1}a_{q-\Delta-1} + a_{q+\Delta}a_{q-\Delta}) + C(a_{q+\Delta-1}a_{q-\Delta} + a_{q+\Delta}a_{q-\Delta-1})], \tag{33}$$

$$S_4 = \sum_{q=0}^{Q}[A(a_{q-1}^2 + a_q^2) + 2C(a_{q-1}a_q)], \tag{34}$$

where $A = \int_0^{T_c} R^2(t)dt = \int_{-T_c}^{0} R^2(t)dt$ and $C = \int_0^{T_c} R(t)R(t+T_c)dt$. Note that $a_l = 0$ for $l > L-1$ or $l < 0$.

From (31)-(34) S_1+S_2 and S_3+S_4 can be expressed as

$$S_1+S_2 = \sum_{q=0}^{Q}[(a_{q+\Delta}+a_{q-\Delta})(Aa_q + Ca_{q-1}) + (a_{q+\Delta-1}+a_{q-\Delta-1})(Aa_{q-1}+Ca_q)], \tag{35}$$

$$S_3+S_4 = \sum_{q=0}^{Q}[A(a_{q-1}^2 + a_q^2 + a_{q+\Delta-1}a_{q-\Delta-1} + a_{q+\Delta}a_{q-\Delta}) + C(2a_{q-1}a_q + a_{q+\Delta-1}a_{q-\Delta} + a_{q+\Delta}a_{q-\Delta-1})]. \tag{36}$$

Note that when $\Delta > L > Q$, the signal part in (18) can be expressed as

$$S_{b_i} = b_i\frac{E_s\alpha}{2}\sum_{q=0}^{Q}[A(a_{q-1}^2+a_q^2) + 2C(a_{q-1}a_q)], \tag{37}$$

which corresponds to the case that no collision occurs between the reference and the data pulses.

The noise term $N = N_1+N_2$ can be shown to be distributed as in (25), where $\sigma_2^2(b_i)$ in (26) is now given by

$$\sigma_2^2(b_i) = \int_{-\infty}^{\infty}[h_{b_i}^2(\tau;0,T_d) + h_{b_i}^2(\tau;T_d,0)]d\tau. \tag{38}$$

Then, the BEP expression is obtained as

$$P_e = 0.5\,Q\left(\frac{0.5E_s\alpha(S_1+S_2+S_3+S_4)}{\sqrt{\frac{\sigma_n^4(Q+1)}{N_f^2}\,\sigma_1^2 + \frac{\sigma_n^2E_s\alpha}{2N_f^3}\,\sigma_2^2(1)}}\right) + 0.5\,Q\left(\frac{0.5E_s\alpha(S_3+S_4-S_1-S_2)}{\sqrt{\frac{\sigma_n^4(Q+1)}{N_f^2}\,\sigma_1^2 + \frac{\sigma_n^2E_s\alpha}{2N_f^3}\,\sigma_2^2(-1)}}\right). \tag{39}$$

D. Simulation Results

In this section, we perform computer simulations in order to study the properties of the proposed hybrid system and verify the theoretical analysis.

In the simulations, we have considered channel models from the IEEE 802.15.3a standard [13]. Those channel models, which were designed for 7.5 GHz bandwidth, are bandpass filtered for a simulation of a 500 MHz wide system. The polarity codes and the TH codes are randomly generated from the sets $\{-1,+1\}$ and $\{0,1,2\}$, respectively[1].

Figure 3 plots the theoretical BEP curves versus signal-to-noise ratio (SNR) for the four different IEEE channel models, CM-1, CM-2, CM-3 and CM-4. For each channel, the integration interval (equivalently Q in (16)) is roughly optimized and the systems are simulated with those optimal Q values. The number frames per symbol, N_f, is 3 and the number of chips per frame, N_c, is 100. The distance between the reference and the date pulse is 50 chips; that is, $\Delta = 50$. From the figure, it is observed that the performance gets worse from CM-1 to CM-4 since the channel spread gets larger,

[1]Since we consider a single-user system, the TH code is generated from a small set for convenience. In fact, the analysis holds for any value of the TH code from the set $\{0,1,\ldots,N_c-Q-2\}$.

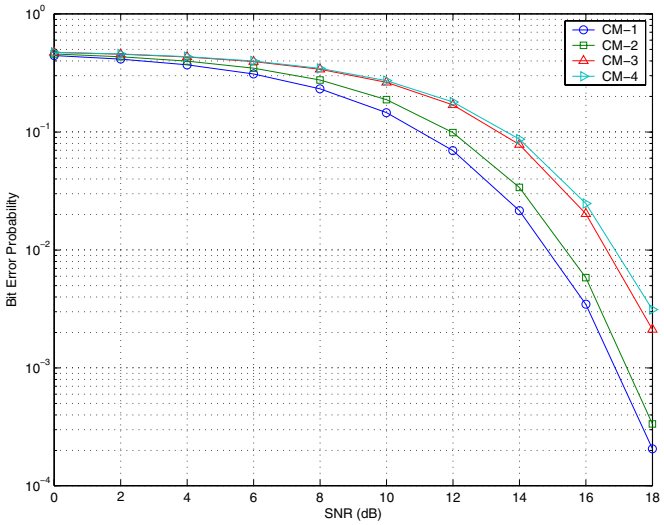

Fig. 3. BEP versus SNR for different IEEE channel models. The parameters are $N_f = 3$, $N_c = 100$ and $\Delta = 50$. $Q = 10, 20, 50, 50$ for CM-1, CM-2, CM-3 and CM-4, respectively. Average BEPs are obtained by means of averaging over 100 channel realizations for each model.

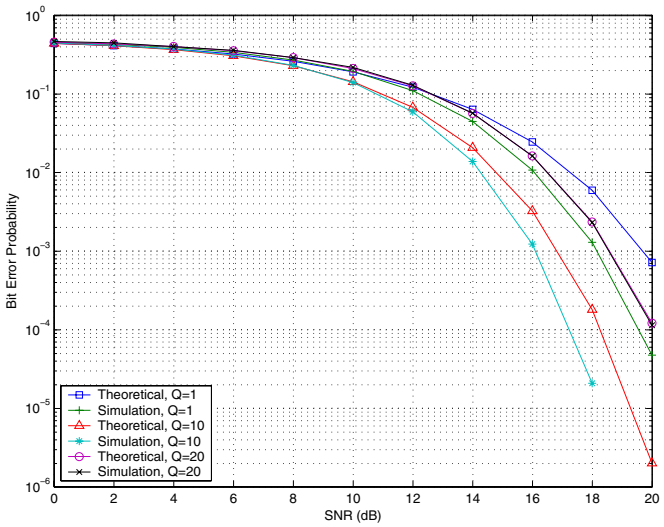

Fig. 4. BEP versus SNR for different Q values. $N_c = 25$, $N_f = 10$ and $\Delta = 12$ and a realization of CM-1 is employed.

which increases the effects of the IFI and reference-to-data pulse interference.

In Figure 4, $N_c = 25$, $N_f = 10$ and $\Delta = 12$ are used, and the theoretical and simulation results are compared for different values of Q for CM-1. We observe that as Q increases the theoretical and simulation results get closer. This is expected since the approximate BEP expression is derived under the condition of large Q values; that is, Lemma 4.1 states that the noise-noise term converges in distribution to a Gaussian random variable as $Q \longrightarrow \infty$.

Using the same parameters as in the previous case, we plot, in Figure 5, the BEP performance of the system in CM-1 for different Q values at SNR $= 18$dB. From the figure, we deduce that for small Q values, the integration interval

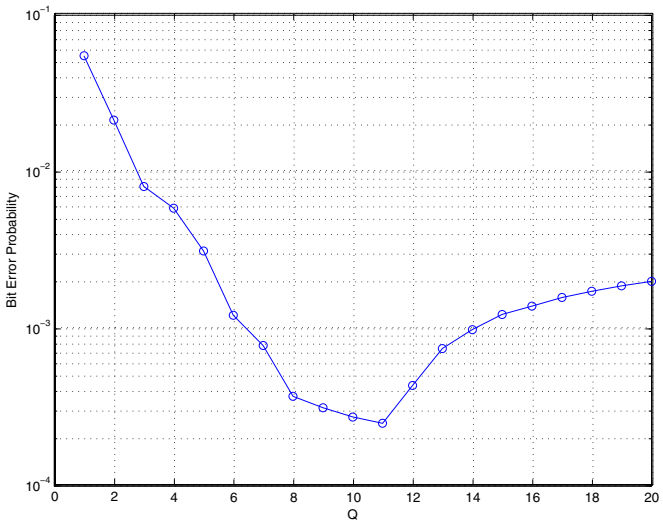

Fig. 5. BEP versus Q at SNR $= 18$. $N_c = 25$, $N_f = 10$ and $\Delta = 12$ are used, and averaging over 100 realizations of CM-1 is performed. The optimal value is $Q = 11$.

is small and therefore very little signal energy is collected. As Q increases to larger values, more signal energy is collected, hence the BEP decreases. However, after a certain point, the collected signal energy becomes less significant than the collected noise-noise and/or interference terms. Therefore, the BEP increases as we increase Q further. From the figure, the optimal value is observed to be at $Q = 11$.

For the next simulations, $Q = \Delta = 12$, SNR $= 18$ and the number of chips per symbol is 512; that is, $N_c N_f = 512$. For a fixed symbol time and energy, the number of frames per symbol is varied and the BEP is plotted in Figure 6 for CM-1. From the plot, it is observed that the frame size does not matter up to the point where IFI becomes dominant. After the frame duration is 16 chips ($N_c = 16$), and thus the IFI becomes significant (due to $\Delta = 12$ and the channel spread), the BEP increases.

For the final simulations, $N_c = 50$, $N_f = 6$ and SNR $= 18$. Figure 7 plots the BEP versus Δ, which is the distance in chips between the reference pulse and the data pulse. As observed from the figure, for small values of Δ, the BEP is high due to the severe interference between the reference and the data pulses. For very large Δ, the BEP is also high since the IFI becomes dominant in that case. Therefore, the optimal value should minimize the total effects of the interference between the reference and data pulses and the pulses from different frames.

V. Concluding Remarks

In the paper we have analyzed a hybrid matched-filter TR correlation receiver. We have found that the impact of the non-Gaussian nature of the noise on the BEP can be significant, and have given the exact closed-form equations for both the resulting variance and the average BEP. We have then analyzed the BEP in multipath environments. Lifting restrictions of previous treatments of the topic, we include the effects of IFI

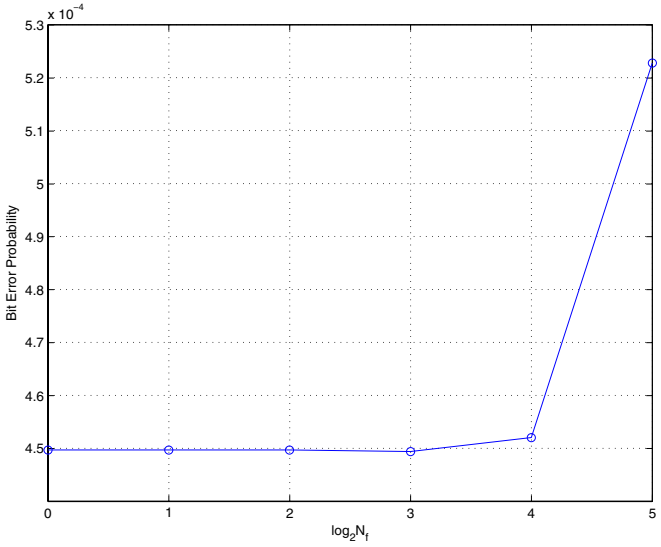

Fig. 6. BEP versus N_f at SNR $= 18$dB. The parameters are $Q = \Delta = 12$ and $N_c N_f = 512$, and CM-1 is considered.

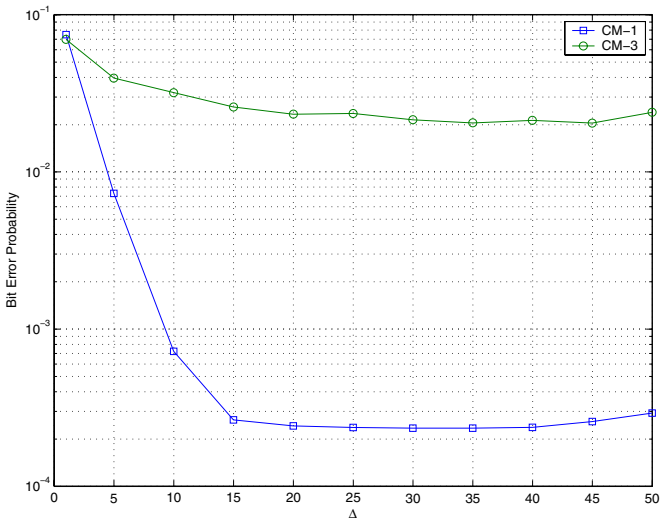

Fig. 7. BEP versus Δ at SNR $= 18$dB. $N_c = 50$ and $N_f = 6$ are used and BEP is averaged over 100 realizations of CM-1 and CM-3.

as well as interference between the reference pulse and the data pulse.

Including the effects of IFI is very important for optimizing the system design of TR systems. Requiring frame durations that are larger than the maximum excess delay of the channel severely restricts the frame rate, and thus the processing gain due to multiple frames, in a TH-IR system. Extremely long frame durations also mean that the peak-to-average ratio of the transmit signal becomes high, which is undesirable both from a hardware point of view, and from a frequency-regulation point of view (note that the FCC report and order [11] limits the admissible peak-to-average ratio).

It is also important to consider the case that the delay between data pulse and reference pulse is smaller than the maximum excess delay of the channel. In many systems, the delay in the receiver is implemented by delay lines. However, it is exceedingly difficult to build delay lines on the order of 10-100ns (typical values for channel maximum excess delays). Therefore, interference between reference pulse and data pulse will occur in practice.

The results of our paper are thus important tools for system design and computational performance of TR UWB systems with practically relevant operating parameters.

REFERENCES

[1] R. A. Scholtz, "Multiple access with time-hopping impulse modulation," *Proc. IEEE Military Communications Conference (MILCOM'93),* vol. 2, pp. 447-450, Bedford, MA, Oct. 1993.

[2] M. Z. Win and R. A. Scholtz, "Ultra-wide bandwidth time-hopping spread-spectrum impulse radio for wireless multiple-access communications," *IEEE Transactions on Communications,* vol. 48, pp. 679-691, Apr. 2000.

[3] M. Z. Win and R. A. Scholtz, "On the energy capture of ultra-wide bandwidth signals in dense multipath environments," *IEEE Communications Letters*, vol. 2, pp. 245-247, Sept, 1998.

[4] D. Cassioli, M. Z. Win, A. F. Molisch and F. Vatelaro, "Performance of low-complexity RAKE reception in a realistic UWB channel," *Proc. IEEE International Conference on Communications (ICC 2002),* vol. 2, pp. 763-767, New York City, NY, Apr. 28-May 2, 2002.

[5] J. D. Choi and W. E. Stark, "Performance of ultra-wideband communications with suboptimal receivers in multipath channels," *IEEE Journal on Selected Areas in Communications,* vol. 20, issue 9, pp. 1754-1766, December 2002.

[6] R. Hoctor and H. Tomlinson, "Delay-hopped transmitted-reference RF communications," *Proceedings of the IEEE Conference of Ultra Wideband Systems and Technologies 2002 (UWBST'02),* pp. 265-269, Baltimore, MD, May 2002.

[7] L. Yang and G. B. Giannakis, "Optimal pilot waveform assisted modulation for ultra-wideband communications," *Proc. the Thirty- Sixth Asilomar Conference on Signals, Systems and Computers,* vol.1, pp. 733-737, Pacific Grove, CA, Nov. 2002.

[8] M. Ho, V. S. Somayazulu, J. Foerster and S. Roy, "A differential detector for an ultra-wideband communications system," *Proc. IEEE Vehicular Technology Conference (VTC 2002 Spring),* pp. 1896-1900, Birmingham, AL, May 2002.

[9] F. Tufvesson and A. F. Molisch, "Ultra-wideband communication using hybrid matched filter correlation receivers," *Proc. IEEE Vehicular Technology Conference (VTC 2004 Spring),* Milan, Italy, May 17-19, 2004.

[10] Y.-P. Nakache and A. F. Molisch, "Spectral shape of UWB signals influence of modulation format, multiple access scheme and pulse shape," *Proceedings of the IEEE Vehicular Technology Conference, (VTC 2003-Spring)*, vol. 4, pp. 2510-2514, Jeju, Korea, April 2003.

[11] Federal Communications Commission, "First Report and Order 02-48," 2002.

[12] F. Tufvesson, S. Gezici and A. F. Molisch, "Ultra-wideband communications using hybrid matched filter correlation receivers," *in preparation*, 2004.

[13] A. F. Molisch, J. R. Foerster and M. Pendergrass, "Channel models for ultrawideband Personal Area Networks," *IEEE Personal Communications Magazine,* vol. 10, pp. 14-21, Dec. 2003.